

Synthesis, characterization, and thermal decomposition of fluorinated salicylaldehyde Schiff base derivatives (salen) and their complexes with copper(II)

Göktürk Avsar · Hüseyin Altinel ·
Mustafa Kemal Yilmaz · Bilgehan Guzel

Received: 30 June 2009 / Accepted: 27 August 2009 / Published online: 11 September 2009
© Akadémiai Kiadó, Budapest, Hungary 2009

Abstract Trifluoromethoxy functionalized copper(II) Schiff base complexes *N,N'*-bis(5-trifluoromethoxysalicylaldehyde)cyclohexanediaminatodiaqua copper(II) and *N,N'*-bis(5-trifluoromethoxysalicylaldehyde)phenylenediaminato copper(II) were synthesized and characterized. Thermal decompositions of the synthesized complexes were studied by thermogravimetry in order to evaluate their thermal stability and thermal decomposition pathways. Three similar decomposition steps occurred for the two copper complexes. Mass losses and evolved gasses were characterized by TG/DTA-MS. Kinetic parameters were calculated and the results showed that the values obtained are comparable.

Keywords Schiff base · Salen · Copper(II) complexes · Thermal decomposition · Coupled TG/DTA-MS

Introduction

Over the past three decades, there have been a number of important advances in the development of general methods for catalytic reactions. Schiff bases derived from salicylaldehyde and diamines, as *N,N'*-bis(salicylaldehyde) ethylenediamine (H_2 -salen), are one of the most important synthetic ligand systems in asymmetric catalysis [1]. Transition metal complexes of salen have been extensively

studied in catalyzing several transformations of organic molecules due to the versatility of their steric and electronic properties [2–4]. Copper(II) complexes of salen have been used in the aziridination and cyclopropanation of olefins and phenol oxidation [5].

Fluorinated derivatives of Schiff base ligands have widely been studied in alternative solvent systems such as bi-phasic reactions and supercritical carbon dioxide ($scCO_2$) due to the solubility properties. $scCO_2$ is emerging as an alternative solvent for various chemical transformations, because it is non-toxic and environmentally benign [6]. Although the structure, $scCO_2$ solubility, and catalytic activity of fluorinated salen were studied previously [7, 8], no thermal decomposition data have been reported in the literatures. Differential thermal analysis (DTA) and thermogravimetric (TG) are useful to study the modes of thermal decompositions as well as the composition of some metal complexes of Schiff bases [9]. This article reports the synthesis, characterization, and detailed thermal decompositions of fluorinated salen copper(II) complexes. The decomposition kinetic parameters such as reaction order, n , the activation energy, E^* , entropies, ΔS^* , and the pre-exponential factor, A , were calculated by using the equation Coats–Redfern of integral method and the equation Horowitz–Metzger of approximation method.

Experimental

Reagent and physical measurements

All chemicals were of reagent grade quality and used as-received. The DTA, TG curves, and mass spectra (MS) are obtained with Perkin-Elmer model working simultaneously with DTA and TG apparatus combined with Pfeifer model

G. Avsar (✉)
Chemistry Department, Faculty of Science and Letters,
Mersin University, 33342 Mersin, Turkey
e-mail: gavsar@mersin.edu.tr; gokturkavasar@yahoo.com

H. Altinel · M. K. Yilmaz · B. Guzel
Chemistry Department, Faculty of Science and Letters,
Çukurova University, 01330 Adana, Turkey

MS system. The heating rate and other characteristics are given as follows: heating rate— 10 K min^{-1} , atmosphere—nitrogen, flow rate of furnace atmosphere— 100 mL min^{-1} , crucible—Platinum, sample size—5–10 mg, reference substance— $\alpha\text{-Al}_2\text{O}_3$.

MS system, Pfeifer model, was used to identify pyrolysis products evolved during heating. IR spectra were recorded on a Perkin-Elmer Mattson 1000 FT-IR spectrometer as KBr pellets in the range of $4000\text{--}400\text{ cm}^{-1}$. Elemental analyses were recorded on a LECO CHNS-932 analyzer for C, H, and N, and Hitachi 180-80 polarized Zeeman Atomic Absorption spectrometer for Cu.

Synthesis

Preparation of the Schiff bases

The fluorinated Schiff base was prepared essentially as described in the literature [10]. For preparation of ligands, an ethanol solution of 2-hydroxy-5-(trifluoromethoxy)benzaldehyde (3.15 mmol) was added dropwise, at room temperature, to a solution of (1R,2R)-cyclohexane-1,2-diamine (for L^1) or 1,2-diaminobenzene (for L^2) (1.55 mmol) in 30 mL ethanol, yielding a large amount of yellow precipitate [2-((E)-((1R,2R)-2-((E)-2-hydroxy-5-(trifluoromethoxy)benzyl ideneamino)cyclohexylimino)methyl)-4-(trifluoromethoxy)phenol = L^1 and 2-((E)-2-((E)-2-hydroxy-5-(trifluoromethoxy)benzylideneamino)phenylimino)methyl)-4-(trifluoromethoxy)phenol = L^2]. The mixture was stirred for 30 min at room temperature and filtered under vacuum. Crystallization from dichloromethane gave the spectroscopically pure product as yellow crystalline compound (yield: 89% for L^1 and 91% for L^2).

Preparation of copper(II) complexes

The copper(II) complexes of L^1 and L^2 were prepared essentially as described in the literature [11]. A solution of 1.2 mmol of $\text{Cu}(\text{AcO})_2 \cdot 4\text{H}_2\text{O}$ in 30 mL EtOH was added to a solution of 1.2 mmol corresponding ligands in 40 mL EtOH at room temperature. The reaction mixture was stirred for 2 h at 80°C . The mixture was concentrated to 20 mL to precipitate the complexes out of the solution (Fig. 1a, b). The crude products were recrystallized from warm dichloromethane (yield: 81% for CuL^1 and 84% for CuL^2).

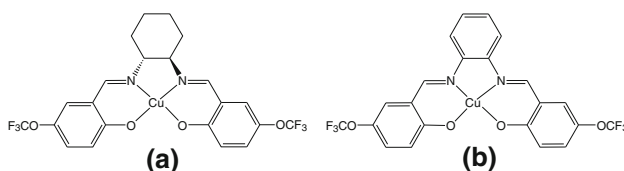


Fig. 1 Structural representations of the complexes: **a** CuL^1 , **b** CuL^2

Table 1 Analytical data for copper(II) complexes

Compound	Found (calc.)/%			
	C	H	N	Cu
CuL^1	44.7 (44.9)	3.8 (3.7)	4.6 (4.7)	10.7 (10.8)
CuL^2	48.3 (48.4)	2.3 (2.2)	4.9 (5.1)	11.6 (11.7)

Table 2 Selected IR data for ligands and complexes (cm^{-1})

Compound	$\nu(-\text{HC}=\text{N})$	$\nu(\text{C}-\text{N})$	$\nu(\text{C}-\text{O})$	$\nu(\text{Cu}-\text{O})$
L^1	1635(s)	1377(m)	1258(s)	—
L^2	1612(s)	1391(m)	1243(s)	—
CuL^1	1596(w)	1417(w)	1313(m)	981(w)
CuL^2	1573(w)	1427(w)	1319(m)	978(w)

s strong, m medium, w weak

The analytical data for the investigated complexes are summarized in Table 1. The calculated values were found to be compatible with the theoretical values. According to the recorded IR spectra, important bands for structural assignments are given in Table 2.

Results and discussion

Characterization of the compounds

The IR spectra of the complexes were compared with salen ligands to obtain the information about binding the ligands to copper in the complexes. The characteristic strong band of the azomethine ($-\text{HC}=\text{N}$) group were observed at $1635\text{--}1612\text{ cm}^{-1}$ in the spectra for free ligands. This band is shifted to the $1596\text{--}1573\text{ cm}^{-1}$ region in the copper complexes, indicating the azomethine–copper coordination as expected [12, 13]. The frequencies of the C–N stretching bands were observed in the 1377 and 1391 cm^{-1} region for ligands and in the region of 1417 and 1427 cm^{-1} for the complexes. These results are in agreement with those of reported values, in the region of $1350\text{--}1410\text{ cm}^{-1}$. The spectra of free ligands show strong bands in the region of $1258\text{--}1243\text{ cm}^{-1}$, assigned to the C–O stretching of the phenol group. However, after complexation of C–O group via oxygen to Cu, these bands observed at the region of $1313\text{--}1319\text{ cm}^{-1}$, indicating the other coordination of the Schiff bases through the phenolic oxygen atom. The band in the 978 and 981 cm^{-1} region is related to the stretching of M–O.

Thermal behavior of complexes

CuL^1 and CuL^2 were studied by thermogravimetric analysis from ambient temperature to 1200°C under nitrogen

atmosphere. The TG curves were redrawn as % mass loss versus temperature, and DTG curves were redrawn as the rate of loss of mass versus temperature. Typical TG, DTG, and DTA curves of CuL¹ and CuL² are presented in Figs. 2 and 3, respectively, and the temperature ranges, percentage mass losses of the decomposition reaction, and the MS cycles are given in Table 3, together with evolved moiety and the theoretical percentage mass losses. All decomposition products were confirmed with simultaneous MS spectra.

There is no detectable change in TG curves up to 300 °C for both CuL¹ and CuL² complexes. The overall losses of mass from the TG curves are 89.97% for CuL¹ and 88.59% for CuL². The complexes show a three-stage mass loss. All decomposition stages were observed as nearly the same, except the first stage mass loss for CuL¹ which was attributed to the release of water.

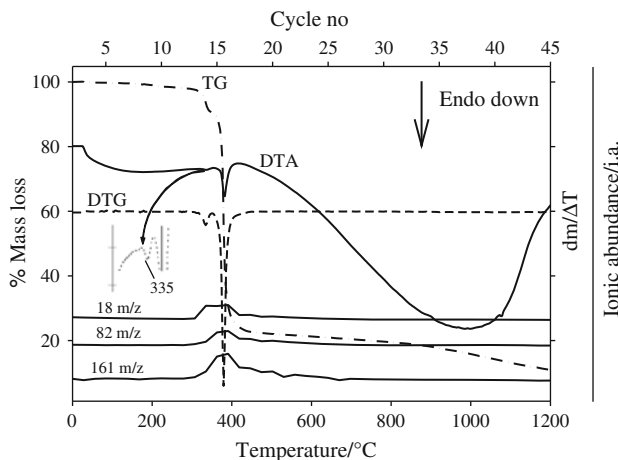


Fig. 2 DTA/TG/DTG-MS curves of CuL¹

Thermal decomposition of CuL¹

The DTA/TG/DTG curves of the compound are shown in Fig. 2. From the TG curve, it appeared that the sample decomposes in three stages over the temperature range 316–1200 °C. As it is seen from the DTA/TG/MS curves that are shown in Fig. 2, the first decomposition occurs at a temperature range between 316 and 353 °C with a mass loss of 6.2% due to the loss of two moles of water, 18 m/z that was confirmed with MS spectra curves corresponding to cycle 14. The second decomposition can be divided into two sub-stages, IIa and IIb, at a temperature range of (starts at 353 °C, ends at 440 °C) 353–392 and 393–440 °C, respectively, with a 68.6% mass loss due to the 2 moles of C₇H₃F₃O, 161 m/z (stage IIa) and C₆H₁₀, 82 m/z (stage IIb) groups assigned to cycle 16 which is agreement with the 68.8% theoretical mass loss. From the DTG curve, there

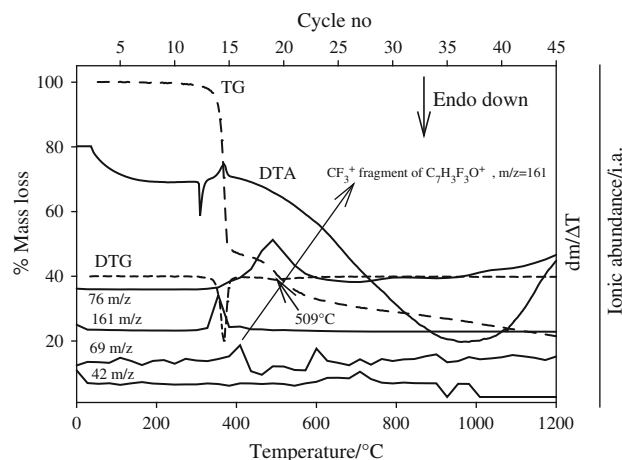


Fig. 3 DTA/TG/DTG-MS curves of CuL²

Table 3 Thermoanalytical results for the investigation compounds

Sample	Stage	Evolved moiety ^a	MS analysis/ m/z ^a	MS cycle no ^a (time)/min	Temperature range		DTG T _{max} /°C	DTA T _{max} /°C	Mass loss found ^a (calc.)/%
					DTG/°C	DTA/°C			
CuL ¹	I	2H ₂ O	18	14 (33.7)	316–353	320–331	335	335	6.22 (6.13)
	IIa	2(C ₇ H ₃ F ₃ O)	161	16 (38.9)	353–392	353–436	376	376	68.64 (68.84)
	IIb	C ₆ H ₁₀	82		393–440				
	III	2(OCN)	42		440–1200	440–1200	—	980, 1090	14.13 (14.21)
	Residue	Cu							11.03 (10.83)
CuL ²	I	2(C ₇ H ₃ F ₃ O)	161	14 (33.7)	328–411	328–410	369	310 melting 369	58.92 (59.09)
	II	C ₆ H ₆	76	19 (46.8)	412–598	411–604	509	—	14.31 (13.95)
	III	2(OCN)	42	27–36 (67.4–90.8)	608–1200	605–1200	—	980, 1090	15.38 (15.41)
	Residue	Cu							11.41 (11.55)

^a According to the simultaneous MS spectra results

are two maxima observed at 335 and 376 °C corresponding to the first and the second mass losses, respectively. And the third stage of mass loss occurs at 440–1200 °C with a mass loss of 14.1% corresponds to the two OCN group. And at the end of decomposition stages, metallic Cu formed as a residue. Three endothermic peaks were noted from the corresponding DTA curve. The first and second peaks were observed at 335 °C as very weak and at 376 °C as sharp maxima, respectively. The third one was observed as a broad peak at the temperature range of 440–1200 °C. All the decomposition steps for the evolved moiety were simultaneously confirmed by MS data shown in Fig. 2, and given in Table 3.

Thermal decomposition of CuL²

From Fig. 3, the TG of CuL² reveals a mass loss in the temperature range 328–1200 °C, corresponding to the formation of Cu as a residue. From the DTA curve, the complex melts at 310 °C, and the first decomposition step starts occurring at the temperature range 328–411 °C, due to the cycle 14. Decomposition product, two moles of C₇H₃F₃O, 161 m/z group with a mass loss of 58.8%, is observed from TG analysis which supported by MS curves. The second decomposition step occurs at the temperature range 412–598 °C due to the formation of Cu(OCN)₂. The decomposition product C₆H₆, 76 m/z group, was confirmed with MS that seen at cycle 19 shown in Fig. 3. And the third mass loss of 15.4% corresponds to the two OCN group, 42 m/z, and at the end of decomposition, metallic Cu formed as a residue. Except the first endothermic peak corresponding to the melting of the compound, one broad endothermic and one exothermic peak were observed in the DTA analysis. The exothermic peak maxima observed at 369 °C corresponding to the first decomposition product. The other broad endothermic peak is in the temperature range of 605–1200 °C. All the decomposition steps for the evolved moiety have also simultaneously been confirmed by MS data and given in Table 3. The increasing ionic abundance at cycle 16 belongs to the curve of 69 m/z may be assigned as CF₃⁺ fragment, which appears after the decomposition product C₇H₃F₃O, 161 m/z.

Decomposition kinetics

Coats–Redfern [14] and Horowitz–Metzger [15] methods were used to calculate the decomposition kinetic parameters. From the TG curves, the order, *n*, activation energy, *E**, entropies, ΔS^* , and pre-exponential factor, *A*, of the thermal decomposition have been elucidated by the well-known methods [14–16].

The linearization curves of Coats–Redfern and Horowitz–Metzger methods are shown in Figs. 4 and 5,

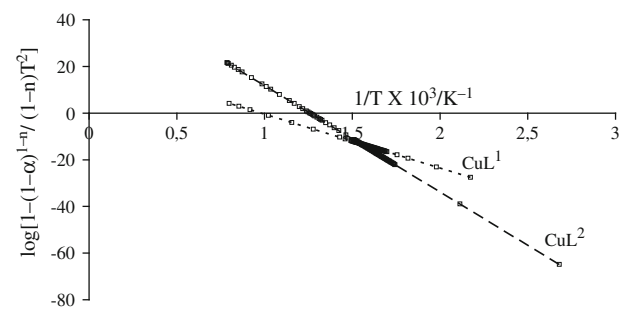


Fig. 4 The linearization curves of Coats–Redfern method of the decomposition stage IIa for CuL¹ and stage I for CuL² complexes

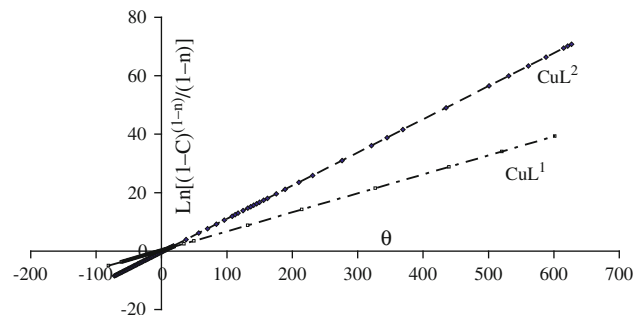


Fig. 5 The linearization curves of Horowitz–Metzger method of the decomposition stage IIa for CuL¹ and stage I for CuL² complexes

Table 4 Kinetic data on the investigated compounds for stage IIa for CuL¹ and for stage I for CuL²

Compounds	Reaction order, <i>n</i>	Parameters	From Coats–Redfern equation	From Horowitz–Metzger equation
CuL ¹	0.815	<i>E*</i>	191.8	228.8
		<i>A</i>	2.515×10^{13}	2.546×10^{16}
		ΔS^*	32.9	62.7
		<i>R</i>	0.9928	0.9924
CuL ²	0.962	<i>E*</i>	379.4	392.6
		<i>A</i>	7.02×10^{28}	1.151×10^{30}
		ΔS^*	328.6	324.2
		<i>R</i>	0.9994	0.9986

Unit of parameters: *E** in kJ mole⁻¹, *A* in s⁻¹, ΔS^* in J mole⁻¹ K⁻¹, *r* correlation coefficient of the linear plot

respectively. Kinetic parameters for the same decomposition stage IIa for CuL¹ and stage I for CuL² calculated by employing the Coats–Redfern and Horowitz–Metzger equations are summarized in Table 4. The results show the values obtained by two methods are comparable.

Conclusions

As a conclusion, the complexes have similar decomposition steps and the kinetic data reached by both of the

methods are in harmony with each other. The activation energies of CuL¹ and CuL² complexes are expected increase in relation with the effect of conjugation (-C=C bond) of the C₆ ring. E* value in the first stage for the CuL² complex is higher than the E* value in the stage of IIa for CuL¹ complex, as expected [17].

The E* values calculated by the method of Coats–Redfern and Horowitz–Metzger for the same decomposition product (C₇H₃F₃O) of the complexes are given in Table 4. The use of these complexes as catalysts in epoxidation reactions in scCO₂ media is still being studied.

Acknowledgements We would like to thank Çukurova University Research Foundation for financial support.

References

1. Ribeiro da Silva MDMC, Gonçalves JM, Silva ALR, Oliveira PCFC, Schröder B, Ribeiro da Silva MAV. Molecular thermochemical study of Ni(II), Cu(II) and Zn(II) complexes with N,N'-bis (salicylaldehydo)ethylenediamine. *J Mol Catal Chem.* 2004;224:207–12.
2. Madhu V, Das SK. Supramolecular π–π assembly of a neutral [Cu(salen)] complex via the templating effect of an ionic inorganic complex Na₂[Cu(mnt)₂] forming a framework type. *Inorg Chem Commun.* 2005;8:1097–100.
3. Serin S, Ispir E. New immobilized Schiff bases synthesis, complexation, characterization and thermal behaviors. *J Therm Anal Calorim.* 2008;94(1):281–8.
4. Ribeiro da Silva MDMC, Araújo NRM, Silva ALR, da Silva LCM, Barros NPSM, Gon-Alves JM, et al. Three N₂O₂ ligands derived from the condensation of 1,2-cyclohexanediamine with salicylaldehyde, acetylacetone and benzoylacetone. *J Therm Anal Calorim.* 2007;87:291–6.
5. Sakthivel A, Sun W, Raudaschl-Sieber G, Chiang AST, Hanzlik M, Kühn FE. Grafting of a tetrahydro-salen copper(II) complex on surface modified mesoporous materials and its catalytic behaviour. *Catal Commun.* 2006;7:302–7.
6. Haas GR, Kolis JW. The diastereoselective epoxidation of olefins in supercritical carbon dioxide. *Tetrahedron Lett.* 1998;39:5923–6.
7. Karabiyik H, Güzel B, Aygün M, Boğa G, Büyükgüngör O. 1-((E)-{(1R,2R)-2-[(E)-(2-Hydroxy-1-naphthyl)methyleneamino]cyclohexyl}iminiomethyl)naphthalen-2-olate: a Schiff base compound having both OH and NH character. *Acta Crystallogr.* 2007;C63:o215–8.
8. Cavazzini M, Manfredi A, Montanari F, Quici S, Pozzi G. Asymmetric epoxidation of alkenes in fluorinated media, catalyzed by second-generation fluorous Chiral (salen)manganese complexes. *Eur J Org Chem.* 2001;24:4639–49.
9. Issa RM, Amer SA, Mansour IA, Abdel-Monsef AI. Thermal studies of bis salicylidene adipic dihydrazone derivatives and their complexes with divalent ions of Mn, Co, Ni, Cu and Zn. *J Therm Anal Calorim.* 2007;90:261–7.
10. Aranha PE, Souza JM, Romera S, Ramos LA, dos Santos MP, Dockal ER, et al. Thermal behavior of vanadyl complexes with Schiff bases derived from trans-N,N'-bis(salicylidene)-1,2-cyclohexadiamine (t-Salcn). *Thermochim Acta.* 2007;453:9–13.
11. Zhou B, Zhou Y, Jiang S, Zhou D. Thermal decomposition of N,N'-ethylenebis(salicylideneiminato) diaquochromium(III) chloride. *Thermochim Acta.* 2000;354:25–30.
12. Thangadurai TD, Ihm S. Chiral Schiff base ruthenium(II) carbonyl complexes: synthesis, characterization, catalytic and antibacterial studies. *Synth React Inorg Met Org Chem.* 2006;36:435–40.
13. Osman AH. Synthesis and characterization of cobalt(II) and nickel(II) complexes of some Schiff bases derived from 3-hydrazino-6-methyl[1,2,4] triazin-5(4H)one. *Transition Met Chem.* 2006;31:35–41.
14. Coats AW, Redfern JP. Kinetic parameters from thermogravimetric data. *Nature.* 1964;201:68–9.
15. Horowitz HH, Metzger G. A new analysis of thermogravimetric traces. *Anal Chem.* 1963;35:1464–8.
16. Arslan H, Özpozan N, Tarkan N. Kinetic analysis of thermogravimetric data of p-toluidino-p-chlorophenylglyoxime and of some complexes. *Thermochim Acta.* 2002;383:69–77.
17. Camps P, Pujol X, Vazquez S, Percas MA, Puigjaner C, Sola L. Cross-coupling of a functionalized highly pyramidalized Alkene: DSC and NMR study of the [2+2] retrocycloaddition of cyclobutane cross products, hyperstability and pyramidalization of the formed dienes. *Tetrahedron.* 2001;57:8511–20.